International Journal of ChemTech Research
CODEN (USA): IJCRGG, ISSN: 0974-4290, ISSN(Online):2455-9555
Vol.12 No.05, pp 141-154, 2019

Investigation of Mechanical, Thermal and Third Order Nonlinear Optical Properties of L-Alanine Cadmium Chloride Single Crystal

J. Ramajothi[1]*, R. Muraleedharan[2], and G.Vinitha[3]

[1*] Department of Physics, Anna University, Chennai- 600025, India
[2]Department of Physics, PRIST University, Thanjavur – 614904, India
[3]School of Advanced Sciences, VIT Chennai, Chennai- 600 127, India

Abstract : The L-alanine cadmium chloride (LACC)nonlinear optical (NLO) material was synthesized and the single crystals were grown by slow evaporation solution growth technique at room temperature. The unit cell parameters and morphology of the grown single crystal has been determined by single crystal XRD. The various functional groups present in the LACC was identified and confirmed by FTIR analysis. The optical properties of the LACC were determined by UV-Vis spectral studies and the band gab energy was calculated (5.2 eV). The photoluminescence spectrum of LACC was analyzed and it shows the maximum emission of violet light in the visible region. The TG/DTA analyzes were performed to determine the thermal stability and the melting point of the LACC was measured as 141°C. The microhardness measurement was carried out using Vicker's hardness tester on (100) plane to find out the Meyer's index number (n). The second harmonic generation (SHG) efficiency measurement was carried out using Kurtz and Perry technique and third order nonlinear optical susceptibility (χ^3) was measured by Z-scan technique (4.09×10^{-6} esu).The laser damage threshold of LACC has been determined (67.142 GW/cm^2) using Nd:YAG laser.
Keywords : Single crystal, energy gap, microhardness, photoluminescence,(χ^3) measurement.

1. Introduction

The NLO crystals are having number of applications in the field of photonics, optoelectronics, optical information processing, optical switching and telecommunications etc. Amino-acid based materials have been proved to be attractive materials for NLO applications because they have large second order nonlinearities, short transparency cutoff wavelength and stable physicochemical properties [1- 4].The NH_2 group of L-alanine is protonated by the COOH group, give rise to NH^{3+} and COO^- group[5, 6]. The semiorganic NLO material LACC have been synthesized and single crystals were grown by solution growth technique. The structure, optical, thermal, mechanical, third order nonlinear optical susceptibility (χ^3) and laser damage threshold properties of LACC single crystal has been reported in this paper.

DOI= http://dx.doi.org/10.20902/IJCTR.2019.120517

2 Synthesis and Crystal Growth

2.1 Synthesis and Solubility of NLO Material

The L-alanine cadmium chloride material was synthesized by using L-alanine (AR grade) and cadmium chloride (AR grade) in the equimolar ratio 1:1. The reaction between L-alanine and cadmium chloride is shown in the following equation.

$$CH_3CHNH_2COOH + CdCl_2 \longrightarrow CH_3CHNH_2COOH.CdCl_2$$

The L-alanine and cadmium chloride was dissolved in distilled water and the solution was kept at water bath at 50°C for 24 hrs. The colorless crystalline salt of LACC with 85% of yield was obtained.The molecular structure of LACC is shown in Fig. 1. The solubility of LACC was carried out in water in the temperatures ranging 30 to 50°C (Fig. 2). The solubility of LACC at 30°C is 12 g/10 ml of water. In ethanol the LACC was not dissolved and the solubility of LACCin water is very high so it has been chosen as the solvent for crystal growth.

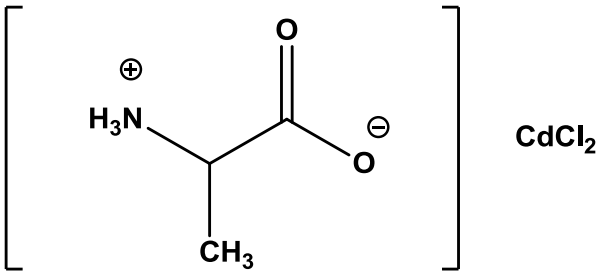

Fig. 1 Molecular structure of LACC.

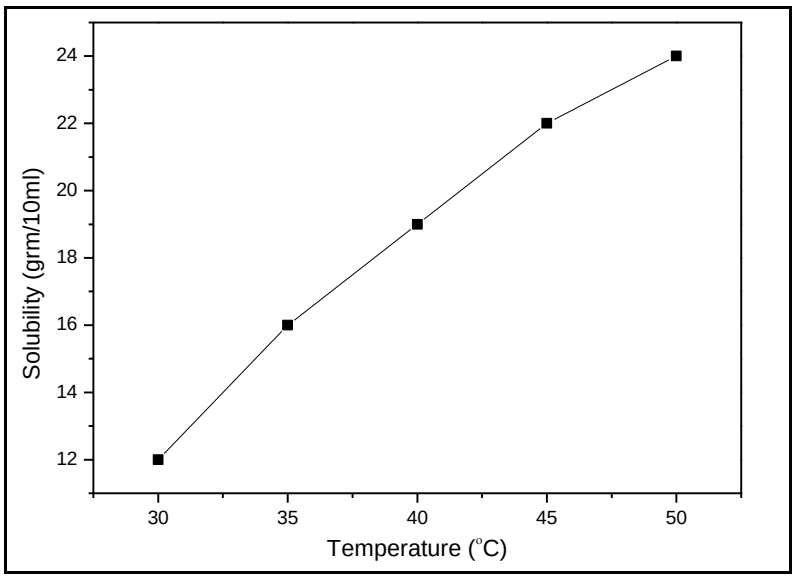

Fig. 2 Solubility curve of LACC.

2.2 Growth of Single Crystal

The synthesized LACC salt was dissolved in distilled water and the solution was stirred well to attain homogeneous mixture in the entire volume of the solution. Then the solution was filtered to remove suspended impurities and this solution was kept at room temperature for slow evaporation to crystallize. The good quality single crystals with a size of 6×15×3 mm^3 were harvested within 20 days with an approximate growth rate of 0.5 mm/day (Fig. 3).

Fig. 3 As grown single crystals of LACC.

3. Characterization Technique

3.1 Single Crystal X-ray Diffraction

The single crystal XRD analysis for LACC crystals were carried out using ENRAF NONIUS CAD-4 single crystal X-ray diffractometer with $M_0K\alpha$ (λ = 0.717 Å) radiation to determine the cell parameters and morphology of the single crystal. The cell parameters of L-alanine cadmium chloride (LACC) was compared with parent material L-alanine (Table.1). The morphology of LACC crystal shows that it has four well developed planes (1 0 0), ($\bar{1}$0 0), (0 0 1), (0 0$\bar{1}$) and these planes are indexed (Fig. 4).

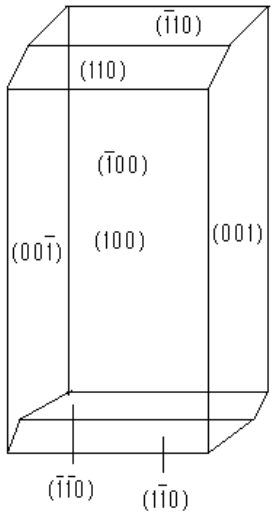

Fig. 4Morphology of LACC single crystal.

Table. 1 Lattice parameters of L-alanine and LACC.

Cell dimensions	L-alanine [7]	L-alanine cadmium chloride (LACC)
a (Å)	6.041	16.18
b (Å)	12.353	7.28
c (Å)	5.774	7.987
α (°)	90	90
β (°)	90	116.75
γ (°)	90	90
V $(Å)^3$	431.12	840
Crystal system	Orthorhombic	Monoclinic

3.2 FTIR Spectral Analysis

The FT-IR spectrum of LACC was recorded using Perkin Elmer spectrometer RXI by KBr pellet technique in the range 400-4000 cm^{-1} (Fig. 5). The NH^{3+} bending vibration at 1620 cm^{-1} of L-alanine is shifted to lower frequency at 1614 cm^{-1} in LACC [8, 9]. The CH_3 symmetric bending vibration was observed at 1355 cm^{-1} in L-alanine. The same vibration bands were observed in LACC at 1345 cm^{-1}[8]. The COO^- bending and rocking vibration of L-alanine are observed at 771 cm^{-1} and 540 cm^{-1} respectively. The same vibration band was shifted to 767 cm^{-1} and 535cm^{-1}in LACC respectively [9,12]. The peak at 3142 cm^{-1} and 3496 cm^{-1} are corresponding to the NH^{3+} symmetric and asymmetric stretching vibration of LACC respectively [8,11]. The sharp peak at 1412 cm^{-1} shows the COO^-symmetric stretching of LACC [9]. The observed frequencies and their assignment are compared with L-alanine (Table.2).

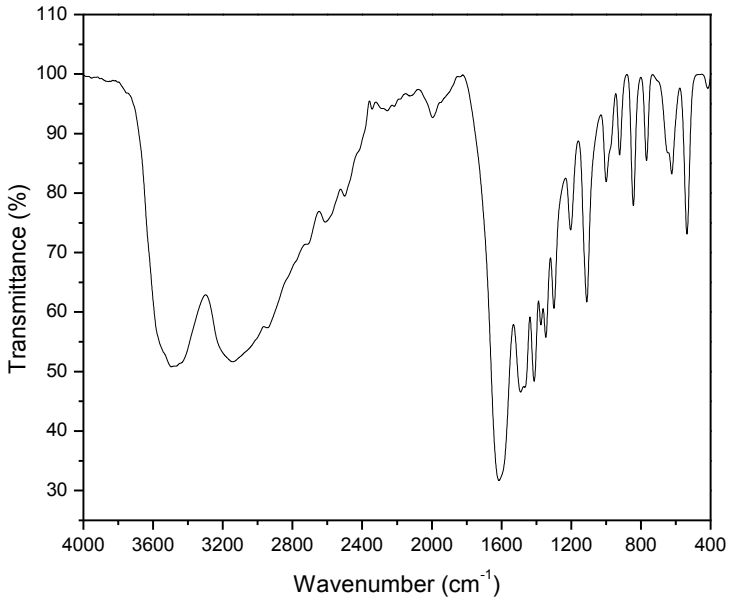

Fig. 5 FT-IR spectrum of LACC.

Table.2 Comparison of IR band with L-alanine.

Wavenumbers (cm^{-1})		**Assignment [8-12]**
L-alanine [8]	**L-alanine cadmium chloride [LACC]**	
3085	3142	ν$_s$ (NH^{3+})
	3496	ν$_{as}$ (NH^{3+})
1620	1614	δ (NH^{3+})
1355	1345	δ$_s$ (CH_3)
1413	1412	ν$_s$ (COO^-)
771	767	δ(COO^-)
648	622	δ(COO^-)
540	535	ρ$_r$(COO^-)
919	922	ν$_s$(C-C-N)
1113	1110	ρ$_r$(NH^{3+})

ν - stretching, δ- bending, s- symmetric, as- asymmetric, ρ_r–rocking

3.3 Study of UV-Vis Transmittance

The UV-Vis spectral transmittance studies of LACC (2 mm thickness) were carried out using lambda UV-Vis spectrophotometer in the range 190-1200 nm (Fig. 6). The transmission study helps to analyze the promotion of electrons to different energy states due to absorption of UV and visible light.The lower cutoff wavelength for LACC is 230 nm and the transmission percentage of 35% in the entire visible and IR region enables for NLO device application [13,14].

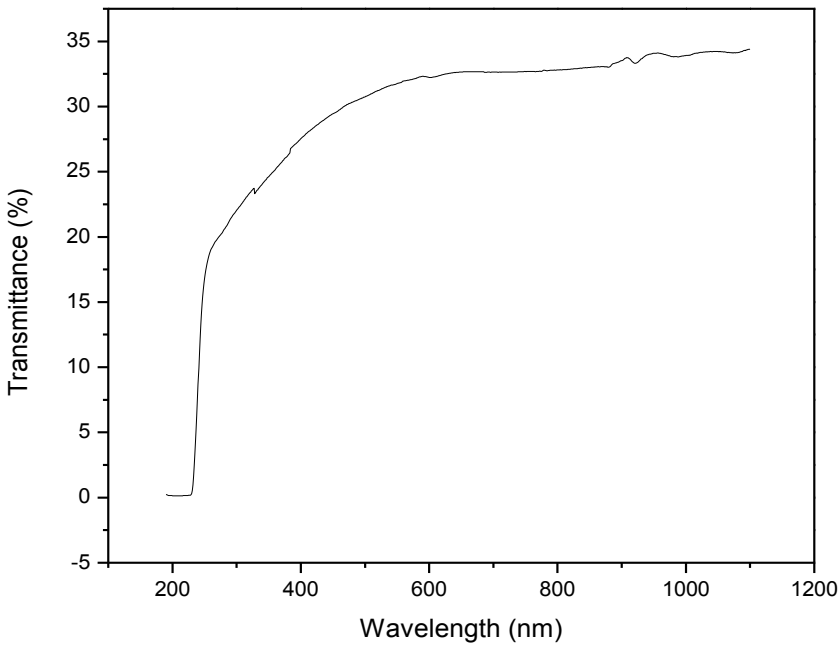

Fig. 6 UV-Vis transmittance spectrum of LACC.

The optical absorption co-efficient (α) was calculated from the transmittance using the following relation (1).

$$\alpha = \frac{2.306 \log\left(\frac{1}{T}\right)}{t} \qquad (1)$$

Where T and t are transmittance and thickness of the crystal respectively. The absorption co-efficient (α) obeys the following relation for high photon energies (hν).

$$\alpha h\nu = A(h\nu - E_g)^{1/2} \qquad (2)$$

'A' is constant, 'E_g' is optical band gap, 'h' is the Planck constant and 'ν' is the frequency of incident photons [15, 16].The band gap of LACC crystal was determined by plotting $(\alpha h\nu)^2$ vs (hν) and extrapolating the linear portion near the on set of absorption edge to the energy axis and then band gap energy is found to be 5.2 eV(Fig. 7). The extinction co-efficient of LACC was calculated from the relation.

$$k = \frac{\alpha\lambda}{4\pi} \qquad (3)$$

The extinction coefficient of LACC was decreases with the increasing photon energy is shown in Fig. 8.

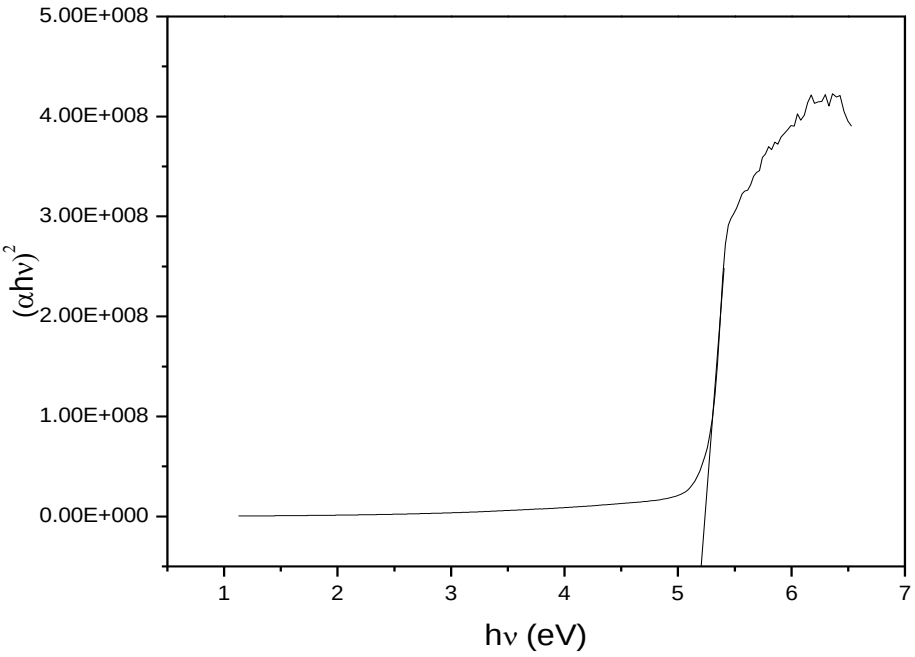

Fig. 7 Tauc's plot of LACC crystal.

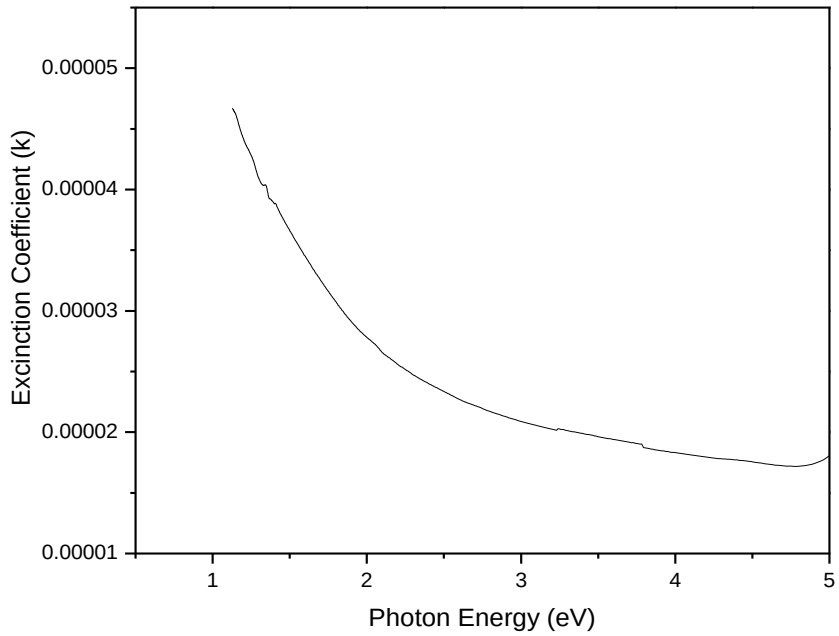

Fig. 8 Photon energy Vs extinction coefficient.

The reflectance was calculated from the equation (4). The reflectance of the LACC increases with the increasing photon energy (Fig. 9).

$$R = \frac{\exp(-\alpha t) \pm \sqrt{\exp(-\alpha t)T - \exp(-3\alpha t)T + \exp(-2\alpha t)T^2}}{\exp(-\alpha t) + \exp(-2\alpha t)T} \qquad (4)$$

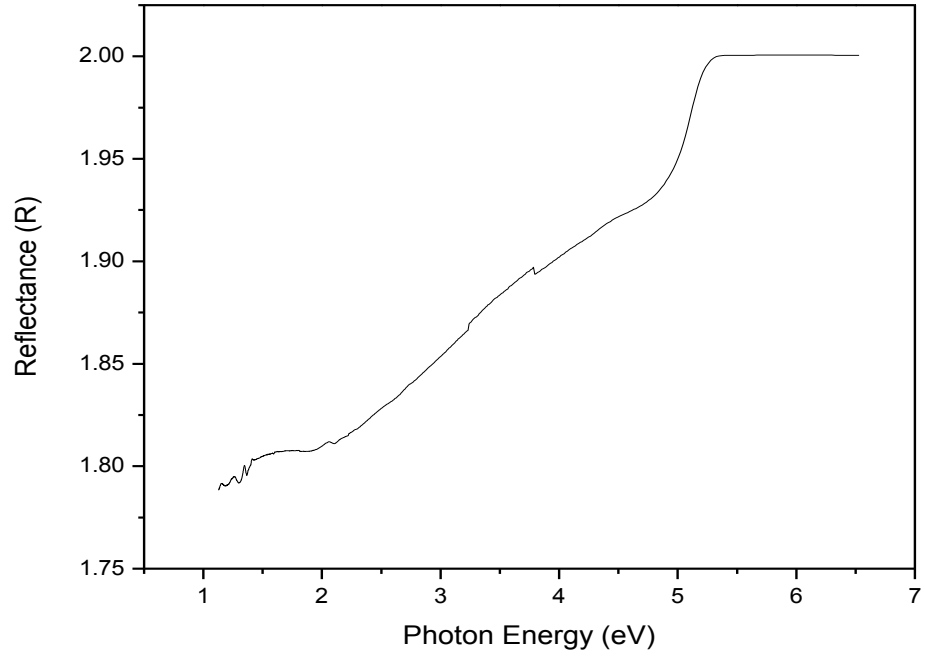

Fig. 9 Photon energy Vs Reflectance.

3.4 Photoluminescence Spectrum

Photoluminescence (PL) is the process of emission of light when photons are excited from ground state. The photoluminescence spectrum of LACC was recorded using Cary eclipse photoluminescence spectroscopy with an excitation wavelength of 240 nm (Fig.10(a)). The spectrum shows that the strong violet emission at 425 nm corresponding energy 3.9 eV (Fig. 10(b)). The weak violet light emission was observed at 450 nm with the energy of 2.6 eV. The peak at 440 nm has the emission of violet light. The peak at 265 nm, 325 nm and 360 nm shows the emission of ultra-violets light have the energy of 4.6 eV, 3.8 eV and 3.4 eV respectively.

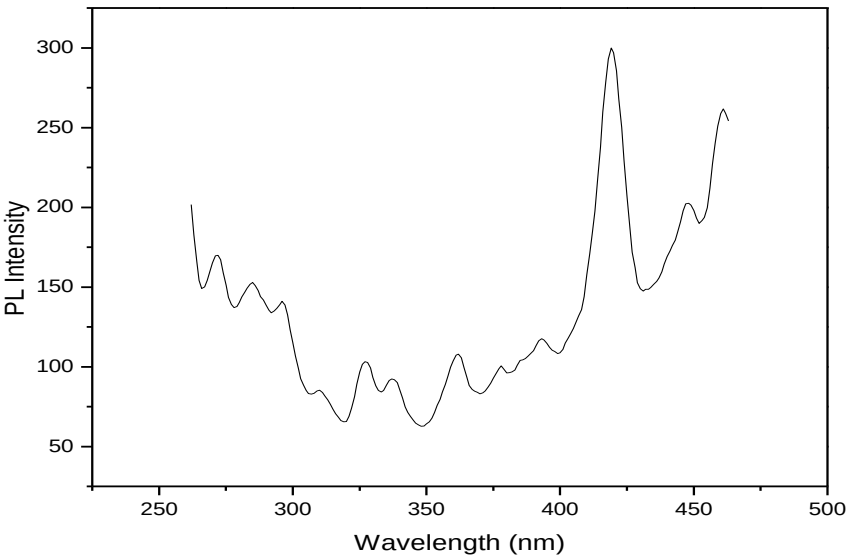

Fig. 10 (a) Photoluminescence (PL) spectrum of LACC.

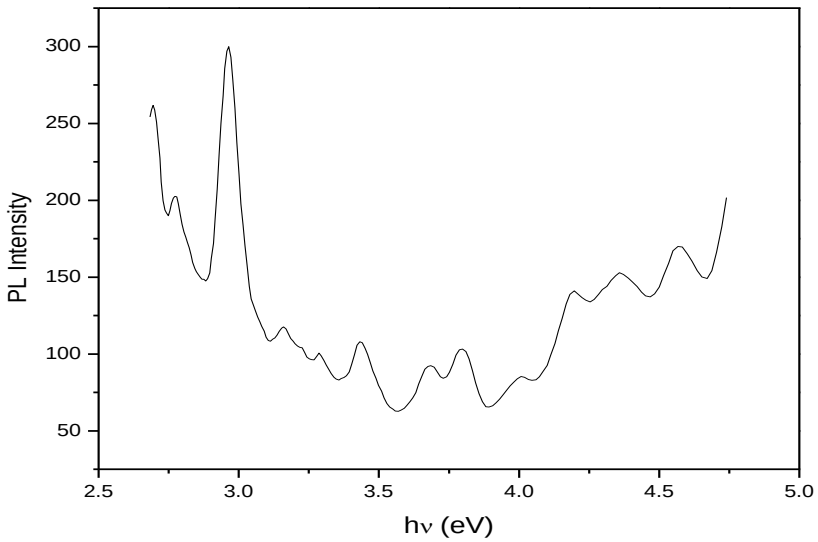

Fig. 10 (b) Photoluminescence (PL) spectrum of LACC in eV.

3.5 Thermal Analyses of LACC

The TGA/DTA analyses were carried out using SDT Q600 for a sample weight of 4.1650 mg in the temperature range 28-1000°C at a heating rate of 10°C/min in the aluminum crucible (Fig. 11). The TGA curve shows that the compound LACC has good thermal stability up to 140°C and there is no weight loss below that temperature and the major weight loss about 30% has been observed in the temperature range 141-350°C. After 350°C, the mass is gradually decrease with the temperature and decomposition of LACC starts above 700°C. The DTA curve shows that melting point of the sample is 141°C.

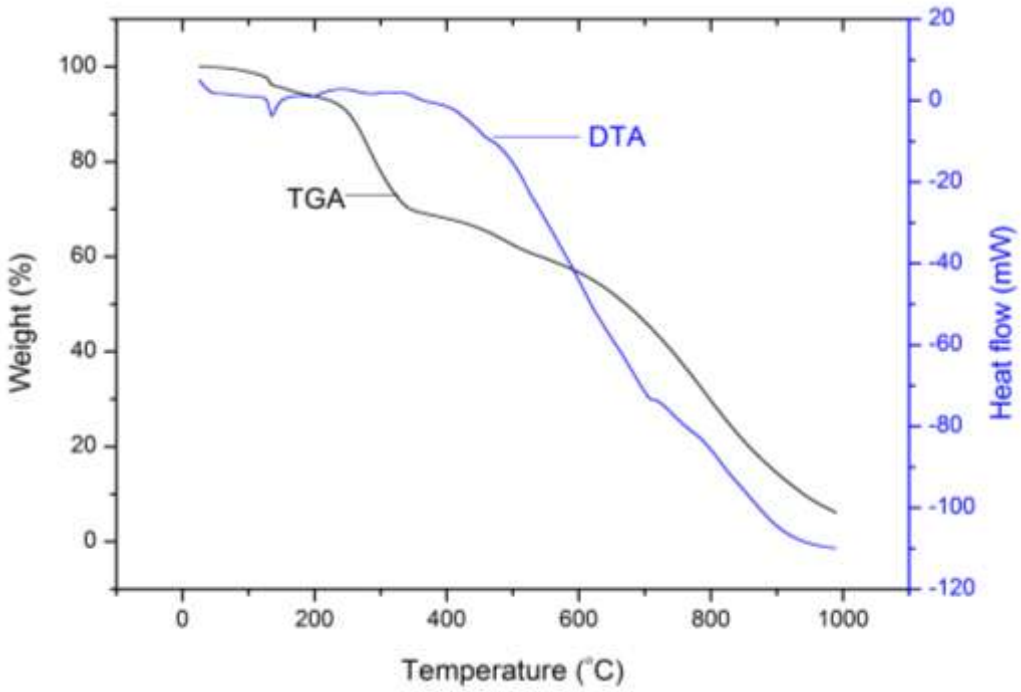

Fig. 11 TG/DTA curves of LACC.

3.6 Determination of Microhardness

Microhardness measurements were carried out using Shimadzu HMV-2fitted with Vicker's pyramidal indenter and attached to an incident light microscope. The grown crystal with well-developed face (100) was

selected for microhardness study. Hardness measurements were taken for applied load varying from 25 to 100 grams keeping the indentation constant at 10 sec. Vicker's microhardness number was determined using the following equation.

$$H_v = \frac{1.8544P}{d^2} Kg/mm^2 \qquad (5)$$

Where P is the indenterload in grams and d is the diagonal length in mm of the impression [15].A graph is plotted between hardness number and applied load from the graph it shows that the hardness of the crystal increases with increasing the applied load (Fig. 12(a)).

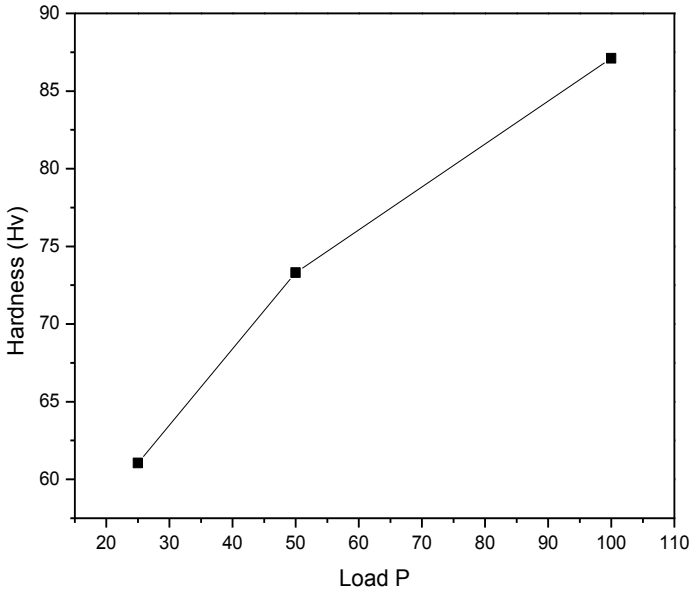

Fig. 12 (a) Variation of hardness with load.

The work hardening co-efficient 'n' was calculated using the following Meyer's law (Fig. 12(b). If "n" should lie between 1 and 1.6 for harder materials and above 1.6 for soft materials [16]. For LACC "n" is 3.52 which indicated that the crystal belongs to soft material category.

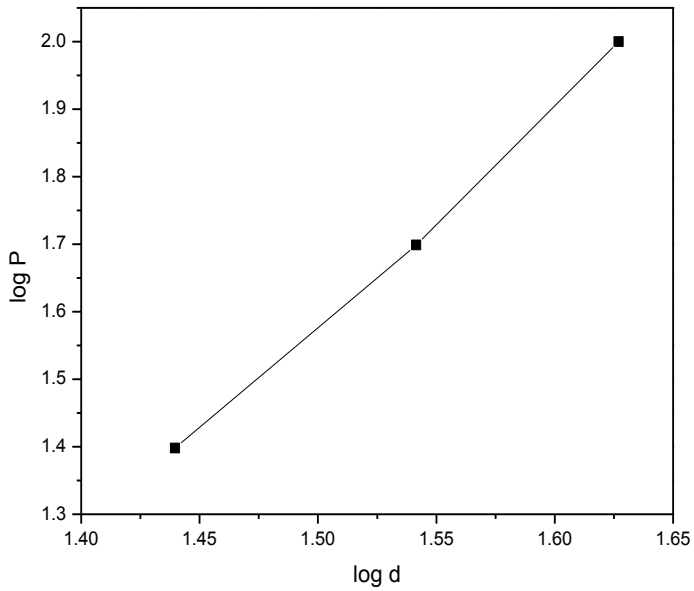

.

Fig. 12 (b) Plot of log d Vs log P.

3.7 Measurement of Second Harmonic Generation (SHG) Efficiency

The SHG efficiency of LACC was determined by Kurtz and Perry technique [18]. The crystal was grounded into a fine powder and densely packed between two transparent glass slides. A Q-switched Nd:YAG laser emitting a fundamental wavelength of 1064 nm (pulse width 8 ns) was allowed to strike the sample. The second harmonic generation in the crystalline sample was confirmed by the emission of green radiation (532nm) emitted by sample. The SHG efficiency of the output signal is found to be 1.2 times that of KDP.

3.8 Determination of Laser Damage Threshold

Laser damage threshold measurement of LACC (4 mm thickness) was carried out for the grown crystal using a Q-switched Nd:YAG laser operating at 1064 nm radiations with 6 ns pulse width and 10 Hz pulse rate [14,18]. The Nd:YAG laser beam was passed along the (1 0 0) direction of LACC crystal. The laser beam of energy around 1.25 mJ to 1.95 mJ, the crystal shows no damage for every 20 s intervals. When the beam with 2.03 mJ was applied on the surface of the crystal it becomes cracked. The microscopic view of before and after damage spot of crystal was shown in Fig. 13. Thelaser damage threshold values of LACC crystal are shown in Table 3. The laser damage threshold of LACC was found to be 67.142 GW/cm^2.

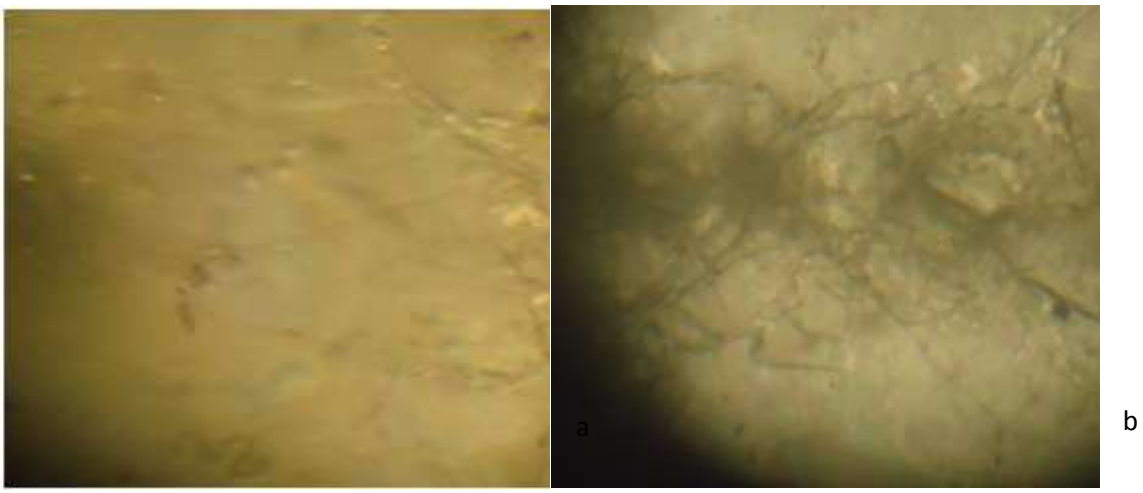

Fig. 13 Microscopic view of before (a) and after (b) damaged spot of LACC.

Table 3 Laser damage threshold of LACC crystal.

Energy (mJ)	No. of Laser pulses	Time (s)	Observation
1.25	20	20	No damage
1.50	20	20	
1.75	20	20	
1.95	20	20	
2.03	20	20	Damaged

3.9 Measurement of THG using Z-Scan Technique

The nonlinear optical transmission of the compounds with and without aperture was measured in the far field as the sample is moved through the focal point. The third-order nonlinear refractive index n_2 and the nonlinear absorption coefficient, of the LACC were evaluated by the Z-scan technique. The Z-scan experiment was performed using a 532 nm diode pumped Nd:YAG (532 nm, 50 mW) laser beam which was focused by a lens with 3.5 cm focal length. The beam waist ω_0 at the focus is measured as 15.84 μm and the Rayleigh length is 1.48 mm [19, 20]. The closed and open aperture of LACC shown in Figs. 15 and 16 respectively. The ratio of open and closed aperture shown in Fig.17 and the nonlinear properties of LACC shown in Table 4.

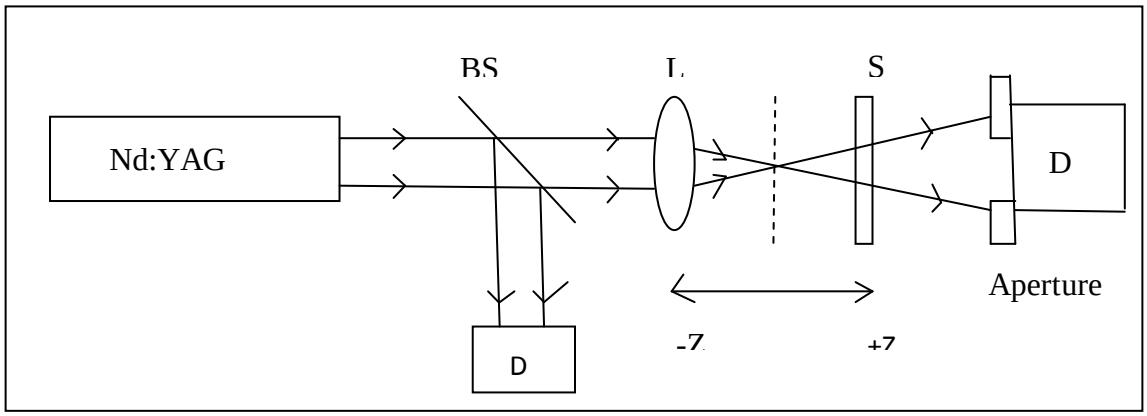

Fig. 14 Schematic experimental setup of Z-scan technique.

A one mm thickness crystal is translated across the focal region along the axial direction that is the direction of the propagation laser beam. The transmission of the beam through an aperture placed in the far field is measured using photo detector and fed to the digital power meter (Field master Gs - coherent). For an open aperture Z-scan, a lens to collect the entire laser beam transmitted through the sample replaced the aperture [21].The Gaussian beam which passes through the sample produces a spatial variation in the refractive index. This makes the sample to behave like a thermal lens resulting in the distortion of the propagating beam. The difference between the normalized peak and valley transmission (ΔTp–v) is written in terms of the on axis phase shift|Δ| at the focus as,

$$\Delta Tp–v= 0.406(1 - S)^{0.25}|\Delta| \quad (6)$$

Where S is the aperture linear transmittance [$S = 1 – \exp(-2r^2_a/w^2_a)$] with r_a is the aperture and ω_a is the beam radius at the aperture [22].The nonlinear refractive index is given by

$$n_2 = V\left(KI_oL_{eff}\right) \quad (7)$$

Where $K = 2\pi/\lambda$ (λ-laser wavelength), I_0 is the intensity of the laser beam at the focus (Z=0), L_{eff} =[1exp(-αL)]/α is the effective thickness of the sample, α is the linear absorption and L is the thickness of the sample.From the open aperture Z-scan data, the nonlinear absorption coefficient is estimated as

$$\beta = \frac{2\sqrt{2}\Delta T}{I_oL_{eff}} \quad (8)$$

The real and imaginary parts of the third order nonlinear optical susceptibility$\chi^{(3)}$can be determined from experimental determination of $n_2$and βaccording to the following relations [23, 24].

$$Re\chi^{(3)} = \frac{10^{-4}(\varepsilon_oC^2n_o{}^2n_2)}{\pi}(cm^2W^{-1}) \quad (9)$$

$$Im\chi^{(3)} = \frac{10^2(\varepsilon_oC^2n_o{}^2\lambda\beta)}{\pi}(cm^2W^{-1}) \quad (10)$$

Where $\varepsilon_o$is the vacuum permittivity $n_o$is the linear refractive index of the sample and c is the velocity of light in vacuum [23]. The value of third order nonlinear optical susceptibility is thus

$$\chi^{(3)} = \sqrt{\left(Re\chi^{(3)}\right)^2 + \left(Im\chi^{(3)}\right)^2} \quad (11)$$

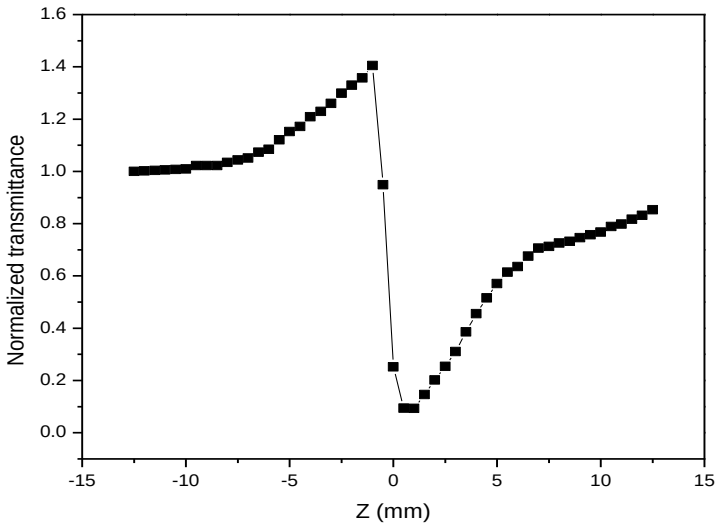

Fig. 15 Closed aperture of LACC.

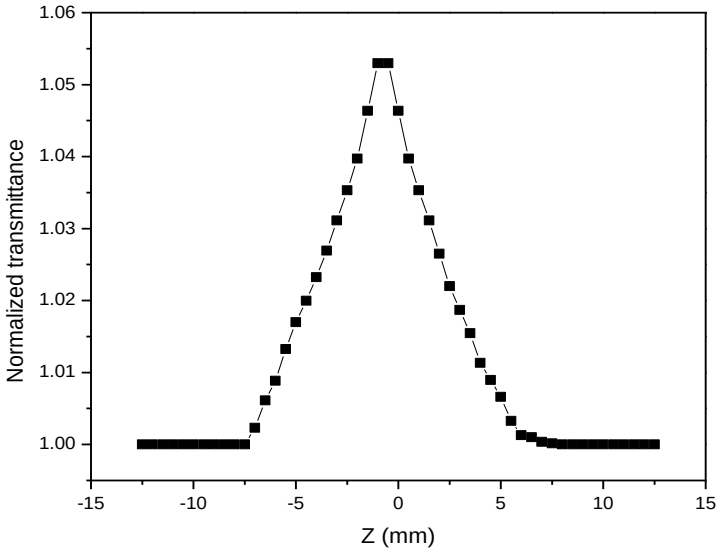

Fig. 16 Open aperture of LACC.

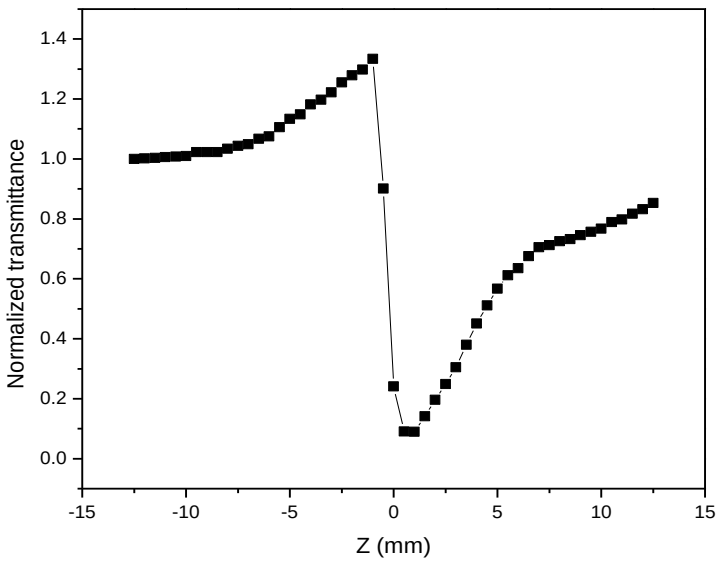

Fig. 17 Ratio of open and closed aperture of LACC.

Table 4 Nonlinear properties of LACC.

Parameters / Crystal	Nonlinear refractive index (n_2)	Nonlinear absorption coefficient (β)	Real part of the third order susceptibility [Re(χ^3)]	Imaginary part of the third order susceptibility [Im(χ^3)]	Third order nonlinear optical susceptibility (χ^3)
LACC	7.29×10^{-8} cm^2/W	1.44×10^{-4} cm/W	4.08×10^{-6} esu	0.27×10^{-6} esu	4.09×10^{-6} esu

4 Conclusion

The semiorganic NLO material of LACC was synthesized and single crystals are grown by slow evaporation method. The single crystal XRD analysis confirmed that LACC crystals were belongs to monoclinic system. The presence of functional groups in LACC was confirmed by FT-IR spectroscopic studies. The transmittance spectrum reveals that the crystal has a low UV cutoff of wavelength with 230 nm and has 35% of transmittance in the entire visible and IR region, enable them for second harmonic generation for various laser sources. The photoluminescence spectrum of LACC shows that maximum violet emission with corresponding energy at 3.9 eV. The TG/DTA revels the good thermal stability of the material. The Vicker's hardness measurement shows that the LACC belongs to soft material category. The SHG efficiency is found that LACC is 1.2 times that of KDP. The crystal LACC was damaged at 2.03 mJ and the third order nonlinear optical susceptibility $\chi^{(3)}$found to be 4.09×10^{-6} esu.These experimental results show that the LACC crystal shows its prominence for NLO device fabrications.

Acknowledgement

The Principal author acknowledges University Grant Commissions (UGC) for UGC-Start-up grant project.

References

1. Dmitriev, V. G., Gurzadyan, G. G. and Nikogosyan, D. N. (1999). Hand book of nonlinear optical crystals. *Springer-Verlag, III Ed*, Berlin.
2. Chemla, D. S. and Zyss, J.(1987). Nonlinear optical properties of organic molecules and crystals. *Academic Press*, Vol. I & II, New York.
3. Gunter, P.(2000). Nonlinear optical effects and materials. *Springer-Verlab*,First Edition, Berlin Heidelberg, Germany.
4. Sutherland,R. L. (2003). Handbook of nonlinear optics.*Marcel DeKker Inc*,II Ed, New York.
5. Chithambaram, V., Jerome Das, S., Arivudai Nambi, R. and Krishnan. S. (2012).Synthesis, growth and characterization of nonlinear optical urea-ammoniumchloride crystals. *Solid State Sciences*, 14, 216-218.
6. Senthilkumar, M. and Ramachandraraja, C.(2012). Growth, structural, spectral and optical studies on pure and L-alanine mixed bisthiourea cadmium bromide (LABTCB) crystals. *Journal of Minerals & Materials Characterization& Engineering*, 11(6), 631-639.
7. Gokul Raj, S. and Ramesh Kumar, G.(2011).Structural and hardness of nonlinear optical L-alanine single crystals.*Adv. Mat. Lett*, 2(3), 176-182.
8. Dhanuskodi, S., Vasantha, K. and Angeli Mary, P. A. (2007).Structural and thermal characterization of a semiorganic NLO material: L-alanine cadmium chloride.*Spectrochim. Acta Mol. Biomol. Spectrosc.*, 66(3), 637-642.
9. Kalaiselvi, P., Alfred Cecil Raj, S. and Vijayan, N. (2013). Linear and nonlinear optical properties of semiorganic single crystal L-alanine cadmium chloride (LACC).*Optik*, (2013), 124(24), 6978-6982.
10. Bright, K. C. and Freeda, T. H. (2010).Growth and characterization of organometallic L-alanine cadmium chloride single crystal by slow evaporation technique. *Physica B: Condensed Matter*, 405(18), 857-3861.

11. Nakamoto, K. (1978). IR Spectra of Inorganic and coordination compounds, IInded., Wiley Interscience, New York.
12. John Coates. (2000). Interpretation of infrared spectra, a practical approach. *John Wiley & Sons Ltd*, Chichester.
13. Ramajothi, J. and Dhanuskodi, S. (2006). Crystal growth, thermal and optical studies on phase matchable new organic NLO material for blue-green laser generation. *J. Cryst. Growth*, 289, 217- 223.
14. Senthil, K., Kalainathan, S., Ruban Kumar, A. and Aravindan, P. G. (2014). Investigation of synthesis, crystal structure and third order NLO properties of a new stilbazolium derivative crystal: a promising material for nonlinear opticaldevices. *RSCAdv*, 4, 56112-56127.
15. Marudhu, G., Krishnan, S, and Vijayaraghavan, G. V. (2014). Optical, theoretical and mechanical studies on sodium acid phthalate crystal. *Optik*, 125, 2417-2421.
16. Krishnan, K., Justin Raj, C., Dinakaran, S., Uthrakumar, R., Robert, R. and Jerome Das, S. (2008). Optical. thermal, dielectric and ferroelectric behavior of sodium acid phthalate (SAP) single crystals. *J. Phys. Chem. Solids*, 69, 2883-2887.
17. Kurtz, S. K. and Perry, T. T. (1968). A powder technique for the evaluation of nonlinear optical materials. *J. Appl. Phys*, 39, 3798-3812.
18. Senthil Pandian, M. and Ramasamy,P.(2012). Sodium sulfanilate dihydrate (SSDH) single crystals grown by conventional slowevaporation and Sankaranarayanan-Ramasamy (SR) method and its comparative characterization analysis. *Mater. Chem. Phys.*, 132, 1019-1028.
19. Thilak, T., Basheer Ahamed, M. and Vinitha, G.(2013). Third order nonlinear optical properties of potassium dichromate single crystals by z-scan technique. *Optik*, 124, 4716-4720.
20. Vinitha, G. and Ramalingam, A. (2008). Single-beam z-scan measurement of the third-order optical nonlinearities of triarylmethane dyes. *Laser Physics*, 18 (10), 1176-1182.
21. Dhanaraj, P. V., Rajesh, N. P., Vinitha, G. and Bhagavannarayana, G. (2011). Crystal structure and characterization of a novel organicopticalcrystal:2-Aminopyridiniumtrichloroacetate. *Mater. Res. Bull.*, 4(6), 726-731.
22. Vinitha, G. and Ramalingam, A.(2008).Nonlinear studies of acid fuchsin dye in liquid and solid media. *Spectrochim. Acta Mol. Biomol. Spectrosc.*, 69, 1160-1164.
23. Vinitha, G., Ramalingam, A. and Palanisamy, P. K. (2007). Nonlinear studies of Pararosaniline dye in liquid and solid media. *Spectrochim. Acta Mol. Biomol. Spectrosc.*, 68, 1-5.

*****